Prime-space fingerprints of superconductors and superfluid helium from a delayed-oscillator locking grammar

C. Agostino[1, *]

[1] *Independent Researcher, Buenos Aires, Argentina*

(Dated: November 16, 2025)

Delayed-oscillator field theory (DOFT) is a speculative framework in which matter and geometry emerge from a dense network of coupled oscillators with finite memory. In this work we do not attempt to justify DOFT as a fundamental description of Nature. Instead we ask a narrower, more practical question: given a DOFT-inspired locking grammar and a minimal correction law, can we describe a heterogeneous collection of superconductors and superfluid helium using a small, fixed set of parameters?

Each material is mapped to an "integer fingerprint" or a "rational fingerprint" whose exponents are fixed by the locking rules and not tuned per material. A universal correction law with parameters (Γ, η) is calibrated once on classical superconducting elements and then reused across families. On an extended dataset including binary, molecular, iron-based and high-pressure superconductors, as well as superfluid ^{4}He, we find that the same (Γ, η) values produce logarithmic residuals with mean ≈ 0 and modest variance within most families. Integer fingerprints show stable prime exponents by family, while rational fingerprints yield narrow, family-specific distributions of denominators q in the range $q \sim 2$–8. High-pressure superconductors and superfluid helium separate cleanly in q, providing a quantitative "prime-space signature" of their macroscopic behaviour within this grammar. A weak next-neighbour coupling parameter κ produces only small, localized improvements concentrated in MgB_2, and leaves the global fingerprints essentially unchanged.

We interpret these patterns as empirical constraints on any delayed-oscillator model that attempts to use a small set of locks to organize the superconducting landscape, rather than as proof of DOFT itself. All code and data required to reproduce the analysis are provided in an open repository.

I. INTRODUCTION

The delayed-oscillator field theory (DOFT) program starts from a simple but aggressive hypothesis: at sufficiently small scales the relevant degrees of freedom are not point particles on a fixed spacetime, but a dense network of coupled oscillators with finite-range delays and memory kernels. In this picture, what we call "space" and "time" emerge from patterns of coherence and decoherence inside that network, and material properties reflect how different collectives lock into a small set of preferred frequency ratios.

In this work we take a deliberately conservative stance: we do not attempt to prove DOFT as a fundamental theory. Instead, we ask a narrower and more practical question: *given a DOFT-inspired locking grammar and a minimal correction law, can we describe a heterogeneous collection of superconductors and superfluid helium with a small, fixed set of parameters?* Concretely, each material is mapped to either an integer fingerprint or a rational fingerprint q, whose exponents are fixed by the locking rules and not adjusted per material. A universal correction law with parameters (Γ, η) is then calibrated on classical metals under weak constraints $(\Gamma \geq 0, \eta \geq 0)$ and reused across families.

From the point of view of conventional condensed-matter theory, this is an unusual modelling choice. Standard approaches start from microscopics (electronic structure, phonon spectra, pairing mechanisms) and build upwards. Here we go the other way: we start from a simple locking grammar in prime-space and ask whether it can describe a curated cross-section of the superconducting landscape without material-by-material tuning. The resulting fingerprints are not proposed as replacements for microscopic theories, but as a coarse, "spectral" summary of how different macroscopic families sit relative to the same discrete lattice of ratios.

Delayed and memoryful dynamics are ubiquitous in climate models, physiological control and nonequilibrium statistical mechanics [1–5]. The DOFT program borrows mathematical tools from that literature but applies them in a different regime: as organizing principles rather than detailed time-domain predictions.

II. METHODS

A. Dataset and macroscopic jumps

Our dataset aggregates superconductors and superfluid helium into a common format. Each row corresponds to a material and a macroscopic "sub-network" (single band, σ, π, or specific vibrational modes under pressure), and includes: critical temperature T_c, superconducting gap Δ, Debye temperature Θ_D, and Fermi energy E_F when available. From these we construct a small set of dimensionless ratios R ("jumps") such as $T_c \to \Delta$, $\Delta \to \Theta_D$, $\Theta_D \to E_F$, and inter-band σ–π jumps for MgB_2 and

* [cesar.agostino@gmail.com]

related systems.

The v6 dataset used here extends a previous run by adding $\mathcal{O}(50)$ additional superconductors, especially in the iron-based and high-pressure families. Classical superconducting elements are used exclusively for calibrating (Γ, η); all other families are held out for testing.

B. DOFT-inspired locking grammar

Each macroscopic jump is assigned to a "lock" on a discrete lattice generated by the first primes $\{2, 3, 5, 7\}$. In the integer case we write

$$R_{\text{lock}} = 2^a 3^b 5^c 7^d, \tag{1}$$

with nonnegative integer exponents (a, b, c, d) constrained by a small set of rules (e.g. maximum total exponent, allowed patterns per family). In the rational case we further write

$$R_{\text{lock}} = p/q, \tag{2}$$

with p, q co-prime and q restricted to a small range ($q \leq 8$ in the present study). For each jump we choose the lock that minimizes the residual under the correction law described below.

The resulting exponent vectors (a, b, c, d) define the *integer fingerprint* of a family, while the distribution of q defines its *rational fingerprint*. We refer to these collectively as "prime-space fingerprints".

C. Universal correction law and calibration

To account for systematic deviations between the ideal locks and the observed ratios, we introduce a simple correction law parametrized by Γ and η. For each observed jump R_{obs} and chosen lock R_{lock} we define a corrected value R_{corr} and a logarithmic residual

$$\ell_\eta = \log_{10}\left(\frac{R_{\text{obs}}}{R_{\text{corr}}}\right), \tag{3}$$

constructed so that $\ell_\eta = 0$ corresponds to perfect agreement with the ideal lock plus universal correction.

The parameters (Γ, η) are calibrated using only classical superconducting elements, with bootstrap resampling and leave-one-out (LOO) influence diagnostics to quantify uncertainty and stability. In the baseline configuration ($w = 800$, prime cutoff $p = 7919$) we obtain

$$\Gamma \sim \mathcal{O}(10^{-17}), \qquad \eta \approx 4 \times 10^{-5}, \tag{4}$$

with narrow bootstrap confidence intervals and modest LOO sensitivity. These values are then *frozen* and reused for all other families.

D. Cluster coupling parameter κ

We also explore a weak coupling parameter κ designed to capture inter-jump correlations inside a material or sub-network. Setting $\kappa = 0$ corresponds to treating each jump independently under the universal correction law, while $\kappa > 0$ allows small shifts in the effective locks driven by neighbouring jumps. In practice, we find that nonzero κ only produces noticeable changes in MgB_2, and leaves both the global residual statistics and the prime-space fingerprints almost unchanged.

III. RESULTS

A. Integer fingerprints by family

Using the baseline configuration ($w = 800, p = 7919$) with $\kappa = 0$, we obtain integer fingerprints for each family by aggregating the exponents (a, b, c, d) across all factorized jumps. Figure 2 shows violin plots of the distributions of a (prime 2) and d (prime 7) for selected families.

Type-I and Type-II superconductors exhibit remarkably stable mean exponent vectors across bootstrap resamples, with typical values $(\langle a\rangle, \langle b\rangle, \langle c\rangle, \langle d\rangle)$ close to $(1.5, 0.8, 0.5, 0.4)$ and $(1.9, 0.6, 0.5, 0.4)$ respectively. High-pressure and iron-based families show distinct patterns, including a nearly pure 2×7 structure in certain iron-based σ subnetworks. We interpret these as "chords" in the prime lattice that characterize each macroscopic family.

B. Rational fingerprints and separation of families

The rational fingerprints focus on the denominators q of the locks chosen at the factorization stage. Figure 3 shows the distribution of q for superfluid helium, high-pressure superconductors, and iron-based superconductors.

Superfluid ^{4}He is clearly distinct: its q distribution is narrow and centred at low values ($q \sim$ 2–2.3). High-pressure superconductors occupy a broader band around $q \sim$ 3–7, while iron-based superconductors are concentrated near $q = 1$. A Mann-Whitney test on q or on selected exponent components identifies a statistically significant separation between high-pressure superconductors and the classical/iron-based families, with a moderate effect size.

C. Residual structure and family-level fingerprints

Figure **??** summarizes the logarithmic residuals ℓ_η by family and sub-network. The mean residuals are close to zero in most groups, with standard deviations at the level expected from the calibration set.

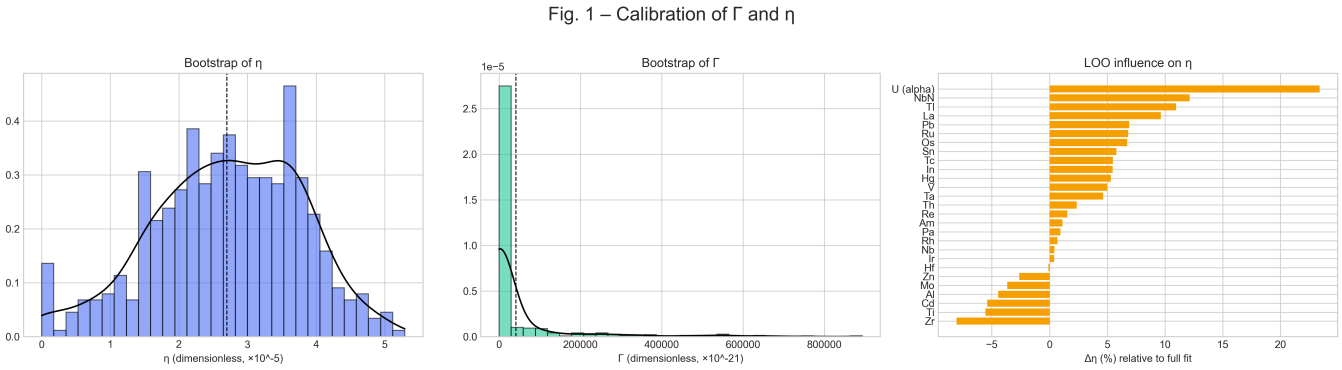

FIG. 1. Calibration of the universal correction parameters (Γ, η) on classical superconducting elements. Left: bootstrap distribution of η. Middle: bootstrap distribution of Γ. Right: leave-one-out (LOO) influence of each element on η, expressed as a percentage shift relative to the full fit.

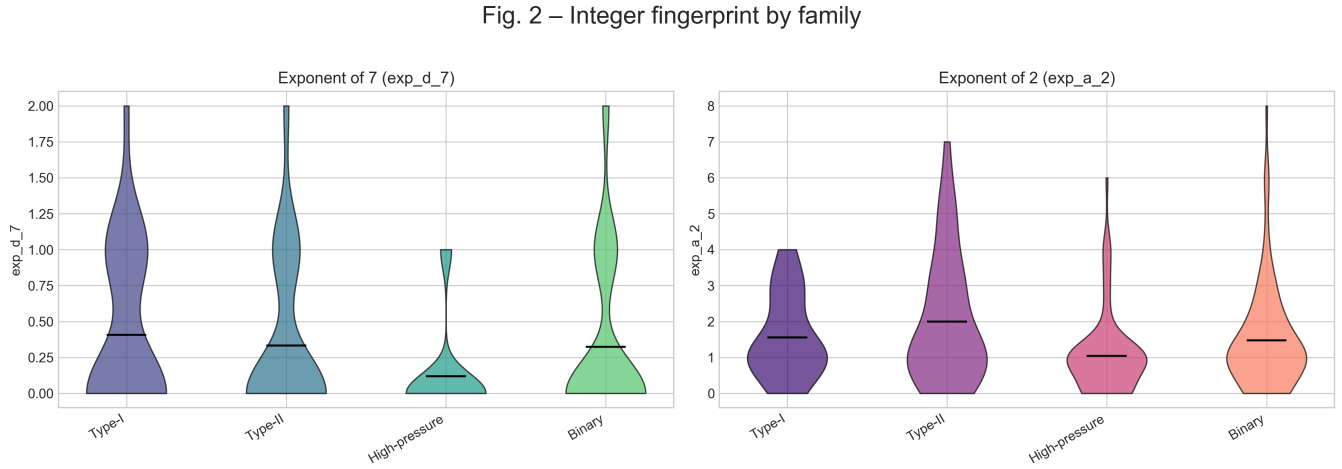

FIG. 2. Integer fingerprints by family. Left: distribution of exponents on prime 7 (d = exp_d_7). Right: distribution of exponents on prime 2 (a = exp_a_2). Each violin summarizes the factorized jumps in that family under the baseline configuration.

Certain groups, notably superfluid helium and a subset of high-pressure modes (e.g. La acoustic σ, H1 optic σ), show systematically negative mean residuals, indicating that the observed ratios sit slightly below the ideal locks plus universal correction. Others, such as binary π-band superconductors and molecular superconductors, show extremely tight residuals around zero. This supports the interpretation that (Γ, η) act as a genuinely universal correction across families, with family-specific structure encoded primarily in the prime-space fingerprints.

D. Effect of the coupling parameter κ

Finally, we compare the baseline $\kappa = 0$ run to a run with small but nonzero κ, using the same $w = 800$ and $p = 7919$. Figure 6 shows the distribution of the difference in post-correction error $\Delta\text{err} = \text{err}_\kappa - \text{err}_\eta$ across all cluster-core jumps, while Figure 7 highlights the ten jumps with the largest $|\Delta\text{err}|$.

Out of the full set of factorized jumps, only a handful—all in MgB_2 σ and π subnetworks—show noticeable changes in the corrected ratios or residuals. For the remaining materials, the choice of κ within the tested range has negligible effect on both the residual statistics and the prime-space fingerprints. Within this grammar, there is therefore no evidence for strong cluster-level couplings beyond the universal correction already captured by (Γ, η).

IV. DISCUSSION AND OUTLOOK

The main outcome of this study is not a new microscopic model of superconductivity, but an empirical statement: a simple locking grammar on the primes $\{2, 3, 5, 7\}$, combined with a universal two-parameter

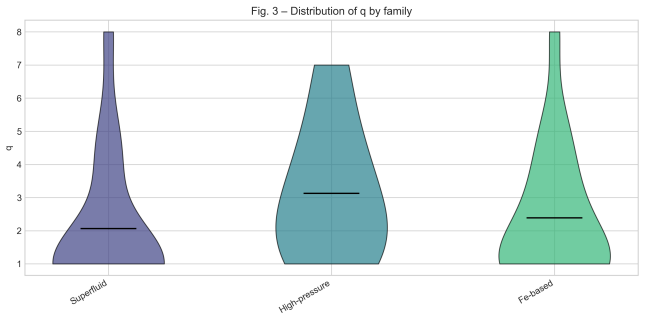

FIG. 3. Rational fingerprints: distribution of denominators q by family (superfluid, high-pressure superconductors, iron-based superconductors). The superfluid cluster sits at low $q \sim 2$–2.3 with a narrow spread, while high-pressure superconductors favour $q \sim 3$–7 and iron-based systems cluster near $q = 1$.

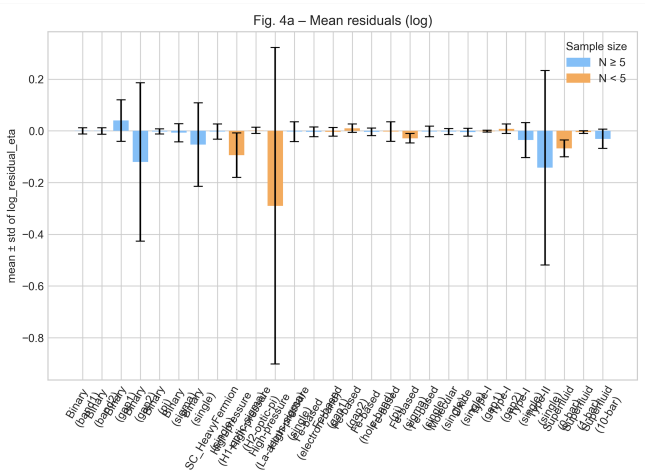

FIG. 4. Mean and standard deviation of the log-residual $\log_{10} r_{\rm obs}/r_{\rm prime}$ for each family and sub-network. Blue bars correspond to groups with $N \geq 5$, orange bars to groups with $N < 5$. Most canonical networks (binary, molecular, iron-based, and high-pressure single) are tightly centered around zero, while superfluid helium and a few high-pressure modes appear systematically compressed (negative mean).

correction law calibrated on classical metals, is sufficient to organize a heterogeneous set of superconductors and superfluid helium into stable prime-space fingerprints. These fingerprints are robust under changes in the dataset (v6 vs. earlier runs), under variation of technical parameters (w and prime cutoff), and under the inclusion of a weak coupling κ.

From a DOFT perspective, this suggests that if a delayed-oscillator network underlies these systems, it may operate with a small, discrete set of preferred ratios and a universal correction that is largely insensitive to microscopic details. From a more conventional perspective, the fingerprints can be viewed as a compact, phenomenological summary of how different families sit relative to the same discrete lattice of scales.

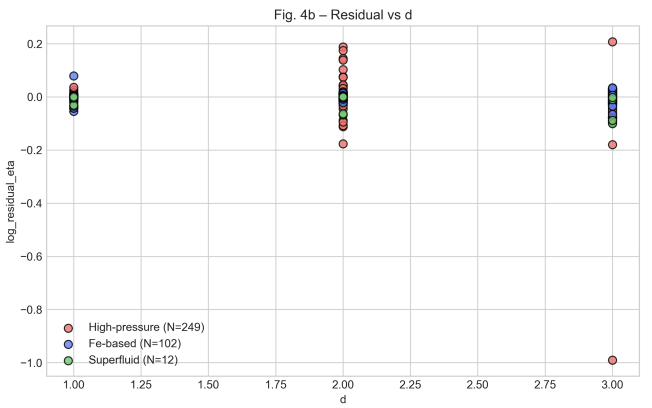

FIG. 5. Scatter of log-residuals $\log_{10} r_{\rm obs}/r_{\rm prime}$ versus the effective dimension d for high-pressure, iron-based, and superfluid networks. The spread remains moderate across $d = 1, 2, 3$, with no runaway tails; most deviations stay within a factor of a few in either direction.

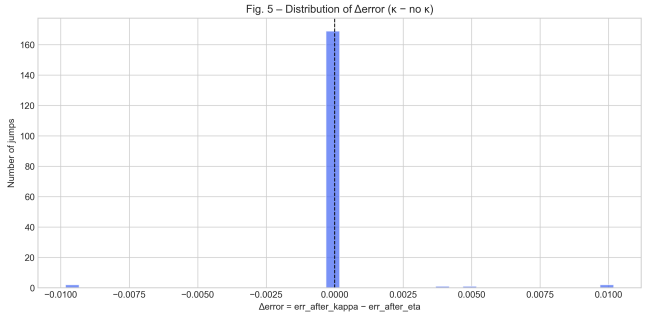

FIG. 6. Distribution of the difference in locking error $\Delta\text{err} = \text{err}_\kappa - \text{err}_\eta$ across all cluster-core jumps. Almost all values lie extremely close to zero, indicating that the κ-correction has negligible effect on the global fit. Only a few jumps in the tails show visible deviations.

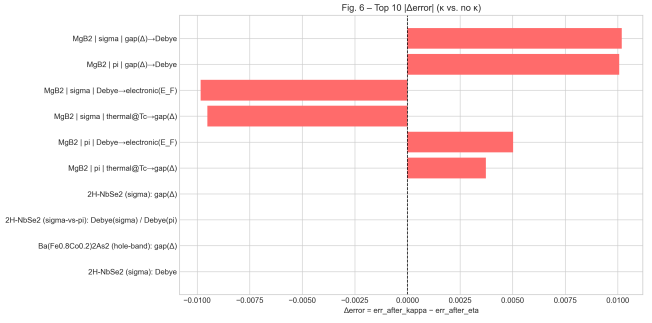

FIG. 7. Largest κ–0 differences in locking error $|\Delta\text{err}| = |\text{err}_\kappa - \text{err}_\eta|$ across cluster-core jumps (top ten). The dominant contributions all come from MgB_2 in its σ and π subnetworks, while only a few non–MgB_2 jumps show much smaller shifts. This confirms that κ mainly refines a handful of multi-gap, strongly coupled cases and leaves the rest of the network essentially unchanged.

We interpret these patterns as the prime-space signature of each macroscopic family under the DOFT-inspired grammar. Whether this signature points to a deeper delayed-oscillator structure, or simply reflects hidden regularities in the curated dataset, is an open question for future work.

ACKNOWLEDGEMENTS

The author thanks colleagues and online communities for discussions and for making high-quality superconductivity and superfluid datasets publicly available. This project made extensive use of open-source software, including Python, NumPy, SciPy, pandas, Matplotlib, and Jupyter.

AI tools were used as assistants in the development of the code and this manuscript. In particular, OpenAI GPT-5.1 Thinking, Google Gemini Pro, and Anthropic Claude were employed for drafting text, refactoring analysis pipelines, and checking statistical procedures. All modelling decisions, dataset curation and interpretations presented here were made and verified by the human author.

[1] H. Mori, Progress of Theoretical Physics **33**, 423 (1965).
[2] R. Zwanzig, *Nonequilibrium Statistical Mechanics* (Oxford University Press, 2001).
[3] B. Efron and R. J. Tibshirani, *An Introduction to the Bootstrap* (Chapman and Hall, 1993).
[4] M. Tinkham, *Introduction to Superconductivity*, Vol. 2 (McGraw-Hill, 1996).
[5] J. Bardeen, L. N. Cooper, and J. R. Schrieffer, Physical Review **108**, 1175 (1957).